Modeling of Membrane Excitability in Gonadotropin-Releasing Hormone-Secreting Hypothalamic Neurons Regulated by Ca^{2+}-Mobilizing and Adenylyl Cyclase-Coupled Receptors

Andrew P. LeBeau,[1] Fredrick Van Goor,[2] Stanko S. Stojilkovic,[2] and Arthur Sherman[1]

[1]*Mathematical Research Branch, National Institute of Diabetes and Digestive and Kidney Diseases, and* [2]*Endocrinology and Reproduction Research Branch, National Institute of Child Health and Human Development, National Institutes of Health, Bethesda, Maryland 20892*

Gonadotropin-releasing hormone (GnRH) secretion from native and immortalized hypothalamic neurons is regulated by endogenous Ca^{2+}-mobilizing and adenylyl cyclase (AC)-coupled receptors. Activation of both receptor types leads to an increase in action potential firing frequency and a rise in the intracellular Ca^{2+} concentration ($[Ca^{2+}]_i$) and neuropeptide secretion. The stimulatory action of Ca^{2+}-mobilizing agonists on voltage-gated Ca^{2+} influx is determined by depletion of the intracellular Ca^{2+} pool, whereas AC agonist-stimulated Ca^{2+} influx occurs independently of stored Ca^{2+} and is controlled by cAMP, possibly through cyclic nucleotide-gated channels. Here, experimental records from immortalized GnRH-secreting neurons are simulated with a mathematical model to determine the requirements for generating complex membrane potential (V_m) and $[Ca^{2+}]_i$ responses to Ca^{2+}-mobilizing and AC agonists. Included in the model are three pacemaker currents: a store-operated Ca^{2+} current (I_{SOC}), an SK-type Ca^{2+}-activated K^+ current (I_{SK}), and an inward current that is modulated by cAMP and $[Ca^{2+}]_i$ (I_d). Spontaneous electrical activity and Ca^{2+} signaling in the model are predominantly controlled by I_d, which is activated by cAMP and inhibited by high $[Ca^{2+}]_i$. Depletion of the intracellular Ca^{2+} pool mimics the receptor-induced activation of I_{SOC} and I_{SK}, leading to an increase in the firing frequency and Ca^{2+} influx after a transient cessation of electrical activity. However, increasing the activity of I_d simulates the experimental response to forskolin-induced activation of AC. Analysis of the behaviors of I_{SOC}, I_d, and I_{SK} in the model reveals the complexity in the interplay of these currents that is necessary to fully account for the experimental results.

Key words: GT1 neurons; mathematical modeling; voltage-gated calcium entry; calcium-mobilization; phospholipase C; adenylyl cyclase

Embryonic and green fluorescent protein-tagged gonadotropin-releasing hormone (GnRH) neurons, as well as immortalized GnRH-secreting neurons (hereafter GT1 cells), display spontaneous action potential (AP) firing (Kusano et al., 1995) as well as fluctuations in intracellular Ca^{2+} concentration ($[Ca^{2+}]_i$) (Constantin and Charles, 1999; Spergel et al., 1999; Van Goor et al., 1999a,b). GnRH secretion from native and immortalized neurons correlates with changes in the pattern of electrical activity (Knobil, 1980; Krsmanovic et al., 1992; Martínez de la Escalera 1992a; Wetsel et al., 1992) and with spontaneous $[Ca^{2+}]_i$ oscillations (Krsmanovic et al., 1992; Terasawa et al., 1999). Both GnRH secretion and oscillations in membrane potential (V_m) and $[Ca^{2+}]_i$ are abolished in Ca^{2+}-deficient medium, demonstrating the dependence of neuropeptide secretion on spontaneous electrical activity. Conversely, AP-driven $[Ca^{2+}]_i$ oscillations and GnRH secretion are facilitated by activating adenylyl cyclase (AC)- and phospholipase C-coupled receptors (Krsmanovic et al., 1991; Martínez de la Escalera et al., 1992b,c; Van Goor et al., 1999a,b).

Experimental identification and characterization of the pacemaker currents underlying AP activity and their modulation by AC- and phospholipase C-coupled receptors in GnRH neurons is incomplete. AC-induced cAMP production occurs in response to dopamine and norepinephrine (Jarry et al., 1990; Martínez de la Escalera 1992b,c; Al-Damluji et al., 1993). In general, cAMP can act indirectly, by modulating various ionic currents in a protein kinase A-dependent manner, or directly, via modulation of cyclic nucleotide-gated (CNG) channels, which have been identified in GT1 neurons (Vitalis et al., 2000). The phospholipase C pathway in GT1 cells is activated by at least two receptors, GnRH and endothelin (Krsmanovic et al., 1991, 1993), leading to Ca^{2+} mobilization from endoplasmic reticulum (ER) stores. As is widely observed in nonexcitable cells (Parekh and Penner, 1997) and in some excitable cells (Bertram et al., 1995; Bennett et al., 1998; Fomina and Nowycky, 1999), including GT1 neurons (Van Goor et al., 1999a), store emptying activates a Ca^{2+}-carrying current (I_{SOC}). When activating both Ca^{2+} mobilization and Ca^{2+} entry pathways in GnRH neurons, communication between the ER and plasma membranes is vital for coordination of responses, with a critical role of I_{SOC} and I_{SK} (Van Goor et al., 1999a). Thus, GT1 cells have a wide repertoire of potential membrane electrical activity and $[Ca^{2+}]_i$ response types, which can be invoked by distinct agonists, and therefore these cells may serve as an excellent experimental and theoretical model for neuroendocrine cells.

One of the major issues that has not been resolved in neuroendocrine cells is the role of multiple Ca^{2+} pools (e.g., cytosol, ER) feeding back to plasma membrane-regulated intracellular signaling. The complexity of such signaling means that determining quantitative consistency between interpretations of experimental records is difficult; although a coherent qualitative representation of the system may be formed, lack of interexperimental constraint means important information may be lost. To address this issue, we have developed a mathematical model of GT1 cell electrophysiology and $[Ca^{2+}]_i$ signaling, allowing simulation of responses to GnRH and other agonists or pharmacological agents.

MATERIALS AND METHODS

GT1 cell culture. All experiments were performed on the GT1–7 subtype of immortalized GnRH neurons (Mellon et al., 1990), which were originally provided by Richard I. Weiner (University of California, San Francisco, CA). The cells were grown in 75 ml culture flasks containing culture medium (DMEM and F-12; 1:1, with L-glutamate, pyridoxine hydrochloride, 2.5 gm/l sodium bicarbonate, 10% heat-inactivated fetal bovine serum, and 100 μg/ml gentamycin; Life Technologies, Grand Island, NY).

Received June 12, 2000; revised Sept. 11, 2000; accepted Sept. 28, 2000.

Correspondence should be addressed to Dr. Andrew LeBeau, Mathematical Research Branch, National Institute of Diabetes and Digestive and Kidney Diseases, National Institutes of Health, BSA Building, Suite 350, 9190 Rockville Pike MSC 2690 Bethesda, MD 20892-2690. E-mail: lebeau@nih.gov.

At confluence, the cells were dispersed by trypsinization (0.05% trypsin) for 10 min, resuspended in culture medium, and plated (50,000 cells/ml) in 35 mm tissue culture dishes (Corning, Corning, NY) with poly-L-lysine-coated (0.01%) coverslips. After incubation for 48 hr, the culture medium was replaced with medium containing B-27 serum-free supplement (Life Technologies) to induce morphological differentiation of the cells. All experiments were performed 3–5 d after serum removal.

Simultaneous measurement of V_m *and* $[Ca^{2+}]_i$. Changes in V_m were monitored using the perforated-patch recording technique, as previously described in Van Goor et al. (1999a). All current-clamp recordings were performed at room temperature using an Axopatch 200 B (Axon Instruments, Foster City, CA) patch-clamp amplifier. Patch pipette tips (3–5 MΩ) were briefly immersed in amphotericin B-free solution containing (in mM): 70 KCl, 70 K-aspartate, 1 $MgCl_2$, and 10 HEPES, pH adjusted to 7.2 with KOH, and then backfilled with the same solution containing amphotericin B (240 μg/ml). To monitor changes in $[Ca^{2+}]_i$, GT1 neurons were incubated for 30 min at 37°C in phenol red-free medium 199 containing Hank's salts, 20 mM sodium bicarbonate, 20 mM HEPES, and 0.5 μM indo-1 AM (Molecular Probes, Eugene, OR). The coverslips with cells were then washed twice with modified Krebs'–Ringer's solution containing (in mM): 120 NaCl, 4.7 KCl, 2.6 $CaCl_2$, 2 $MgCl_2$, 0.7 $MgSO_4$, 10 HEPES, and 10 glucose, pH adjusted to 7.4 with NaOH, and mounted on the stage of an inverted epifluorescence microscope (Nikon). A photon counter system (Nikon) was used to simultaneously measure the intensity of light emitted at 405 and at 480 nm after excitation at 340 nm. Background intensity at each emission wavelength was corrected. The data were digitized at 4 kHz using a personal computer equipped with the Clampex 8 software package in conjunction with a Digidata 1200 analog-to-digital converter (Axon Instruments).

$[Ca^{2+}]_i$ was calibrated *in vivo* according to Kao (1994). Briefly, R_{min} was determined by exposing the cells to 10 μM Br-A23187 in the presence of Krebs'-Ringer's solution with 2 mM EGTA and 0 Ca^{2+} for 60 min; 15 mM Ca^{2+} was then added to determine R_{max}. The values used for the $[Ca^{2+}]_i$ calibration parameters: R_{min}, R_{max}, $S_{f,480}/S_{b,480}$, and K_d were 0.472, 3.634, 3.187, and 230 nM, respectively (for details, see Kao 1994). All reported V_m were corrected for a liquid junction potential between the pipette and bath solution of +10 mV. The bath contained <500 μl of saline and was continuously perfused at a rate of 2 ml/min using a gravity-driven superfusion system. The outflow was placed near the cell, resulting in complete solution exchange around the cell within 2 sec. A solid Ag–AgCl reference electrode was connected to the bath via a 3 M KCl agar bridge. In some experiments, the cells were preloaded with the membrane-permeant Ca^{2+} chelator BAPTA-AM (1 μM) for 45 min at 37°C.

GT1 cell model. We have previously published a GT1 cell model (Van Goor et al., 2000) that included fast, voltage-dependent currents (I_{Na}, I_{CaL}, I_{CaT}, I_{KDR}, I_M, I_{ir} and a linear depolarizing leak current, see the online Appendix at http://www.jneurosci.org), but no $[Ca^{2+}]_i$, $[Ca^{2+}]_{er}$, or $[Ca^{2+}]$-dependent currents. Except for the leak current, the extended model presented here keeps all the fast currents exactly as used in Van Goor et al. (2000). From Van Goor et al. (1999a) we have experimental evidence for I_{SOC} activity in GT1 neurons, and therefore such a current was added. Also, as described in Results, interpretation of the experimental data led us to hypothesize that the leak current (I_d) is a Ca^{2+}-inactivated nonspecific cation current, which is described below. I_{SK} was also added, the parameters for which were derived from experimental data (Van Goor et al., 1999a).

Initially, the Ca^{2+} dynamics were modeled as a simple one-compartment cytosol with a spatially homogeneous $[Ca^{2+}]_{is}$ interacting with a similarly defined ER compartment and a constant $[Ca^{2+}]$ extracellular compartment (see Appendix). The ER was 10% of the total cell volume (the rest being cytosol—no allowance was made for the nucleus or other subcompartments), distributed evenly throughout the total volume. However, it became apparent that to accurately simulate the experimental results it was necessary to subdivide each of the cytosolic and ER pools to allow compartmentalization of Ca^{2+} dynamics in the region at the inner face of the plasma membrane. We refer to the subdivided regions as the "shell" and the "bulk" compartments. The shell represents the 80-nm-deep region (see below) of the cytosol immediately adjacent to the plasma membrane. The bulk represents the rest of the cell interior, ~97.8% of the total volume. There is no physical barrier separating the shell and bulk compartments, and Ca^{2+} is exchanged in a manner and at a rate representing simple diffusion. Each compartment contains the same ratio of cytosol and ER as described above. Thus, there are four distinct pools of intracellular Ca^{2+} with concentrations given by: shell cytosolic $[Ca^{2+}]$ ($[Ca^{2+}]_{is}$), bulk cytosolic $[Ca^{2+}]$ ($[Ca^{2+}]_{ib}$), shell ER $[Ca^{2+}]$ ($[Ca^{2+}]_{ers}$), and bulk ER $[Ca^{2+}]$ ($[Ca^{2+}]_{erb}$). Because the bulk compartment represents almost 98% of the total volume, $[Ca^{2+}]_{ib}$ corresponds to $[Ca^{2+}]_i$ reported by the fluorescent dye in the experimental traces.

The choice of 80 nm for the depth of the shell was based on two criteria: (1) that the volume of the shell be small enough to provide a clear separation in the $[Ca^{2+}]_i$ time scales in the shell and bulk compartments, and (2) that the depth of the shell be sufficient to encompass the outer regions of the ER, including the proposed IP_3 receptor–SOC channel complex (see below). The value of 80 nm fulfills both criteria. In early trial simulations, a value of ~400 nm was also used, and this gave similar results to those for 80 nm, indicating that the value for shell depth used here is not critical.

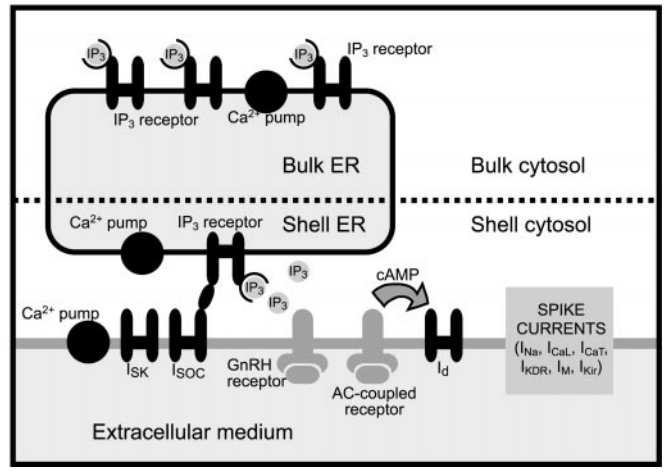

Figure 1. Schematic diagram of the key elements of the model, showing the separation of both the cytosolic and ER pools into shell and bulk compartments and the three pacemaker currents, I_{SK}, I_{SOC}, and I_d. I_{SOC} is thought to be activated via a direct coupling to shell IP_3 receptors (see Materials and Methods for details), whereas I_d is activated by cAMP. A rise in shell $[Ca^{2+}]_i$ activates I_{SK} and inactivates I_d. An animated version of this diagram may be viewed at http://mrb.niddk.nih.gov/alebeau/gt1.html.

Within each pool, Ca^{2+} is 99% buffered, and the given Ca^{2+} concentrations represent free (i.e., unbuffered) Ca^{2+} (see Appendix). Ca^{2+} is pumped out of the cell via plasma membrane pumps (Ca-ATPase and Na^+/Ca^{2+} exchanger) and into the ER by sarcoendoplasmic ATPase (SERCA) pumps. Ca^{2+} release from the ER into the cytosol is modeled by a simple term given as the product of a constant (though adjustable) efflux rate and the difference between the ER and cytosolic $[Ca^{2+}]$. GnRH application is simulated by increasing the efflux rate above its low, resting value. We found that this simple system was sufficient to simulate the effects of IP_3-induced mobilization of stored Ca^{2+} and that a specific description of IP_3 receptor and its kinetics was not necessary. Our simple system does not distinguish whether basal release of stored Ca^{2+} is via IP_3 receptors activated by resting IP_3 levels or via a separate leak pathway.

It was also necessary to include mitochondrial Ca^{2+} handling. Again, uptake was modeled as being via a Ca^{2+} pump. Pivovarova et al. (1999) have provided evidence that excess Ca^{2+} taken into the ER is stored as a precipitate, which means that the free intramitochondrial $[Ca^{2+}]$, and therefore passive release of mitochondrial Ca^{2+}, may be fairly constant. This assumption allows us to dispense with equations governing mitochondrial $[Ca^{2+}]$, retaining just the flux terms in the $[Ca^{2+}]_i$ equations (see Appendix). To accurately reproduce the experimental records, particularly the response to SERCA pump inhibition by thapsigargin (Tg), it was necessary to have higher mitochondrial activity in the shell compartment than in the bulk. This is consistent with reports of localization of mitochondria near the plasma membrane in neurons (Pivovarova et al., 1999) and with ER membranes (Rizzuto et al., 1993; Csordás et al., 1999).

I_{SK} was modeled in the usual way as a product of a macroscopic conductance, fractional activation by $[Ca^{2+}]_{is}$, and a linear voltage driving force (see Appendix for details). I_{SOC} was similarly defined, but with a fractional activation that was inversely related to $[Ca^{2+}]_{ers}$, consistent with a recent report suggesting that activation of I_{SOC} may be specifically regulated by subcompartments of the ER (Broad et al., 1999). Moreover, several other recent reports have suggested that I_{SOC} is activated via a direct coupling with IP_3 receptors in the ER membrane (Kiselyov et al., 1998, 1999; Boulay et al., 1999; Ma et al., 2000) (also see Putney, 1999). The details of such an interaction have not been determined, and so we do not specifically implement this effect. However, our description of I_{SOC} regulation is compatible with such a mechanism.

A schematic diagram of the key elements of the model is given in Figure 1. An animated version may be viewed at http://mrb.niddk.nih.gov/alebeau.

RESULTS

We start by describing five experimental records and reviewing published results, the interpretation of which provides a qualitative understanding of electrical activity and Ca^{2+} signaling in GT1 cells. Our goal is to characterize the roles of the previously described I_{SK} and I_{SOC} in regulating pacemaking in spontaneously and GnRH-induced activity and to determine whether these channels are sufficient to explain the basal and agonist-induced effects. We then test this understanding by simulating the experimental traces with the model. The experimental records and simulations are presented in five figures in which the layout and, as much as

practical, the scaling were kept constant to allow direct comparison between the respective results.

Experimental results

As described previously (Van Goor et al., 1999a), unstimulated GT1 cells fired spontaneous APs at a frequency of ~0.5–1.0 Hz. GnRH application induced a transient hyperpolarization and cessation of AP firing (Fig. 2*A*) and a spike rise in $[Ca^{2+}]_i$ (Fig. 2*B*) caused by IP_3-mediated emptying of the ER Ca^{2+} store. Subsequently, $[Ca^{2+}]_i$ fell to a plateau level that was higher than the prestimulus level, the V_m depolarized, and AP activity resumed with an increased firing rate and decreased amplitude.

Application of apamin, an I_{SK} blocker, completely prevented GnRH-induced hyperpolarization (Fig. 3*A*). When added during the sustained phase of GnRH stimulation, apamin caused an increase in the AP firing space (Van Goor et al., 1999a), whereas in spontaneously active cells, apamin was ineffective. These results indicate that the spike and plateau elevations in $[Ca^{2+}]_i$, but not basal $[Ca^{2+}]_{i,}$ are sufficient to activate SK channels. The results further indicate that the increase in firing frequency after GnRH occurs despite an increase in I_{SK} activity. Thus, activation of a depolarizing current or inhibition of a hyperpolarizing current is needed to overcome the negative effects of activated SK channels on pacemaking.

Several lines of observations indicate that store emptying activates I_{SOC} in GT1 neurons, which may account for this agonist-induced increase in firing frequency (Van Goor et al., 1999a). As shown in Figure 4*B*, Tg, a blocker of SERCA pumps, caused a slow rise in $[Ca^{2+}]_i$, presumably reflecting a slow depletion of the ER Ca^{2+} stores, in contrast to the rapid release of Ca^{2+} observed in GnRH-stimulated cells (Fig. 2*B*). This may account for the inability of Tg to induce a transient hyperpolarization and cessation of AP firing (Fig. 4*A*). Consistent with a role of I_{SOC} in control of pacemaker activity, Tg was also able to induce a sustained increase in the firing frequency. Together, the results in Figures 2–4 suggest that I_{SOC} and I_{SK} act coordinately to regulate AP activity during the response to GnRH, with I_{SOC} overcoming the hyperpolarizing effects of the I_{SK} to increase AP firing rate.

However, the cessation of AP activity, which persisted even when SK channels were blocked by apamin (Fig. 3*A*), cannot be explained by a change in I_{SOC} activity (unless I_{SOC} is sensitive to $[Ca^{2+}]_i$; see Discussion). Activation of I_{SOC} may be delayed if total store emptying is required, but a delay in I_{SOC} activation should lead to a slow increase in firing rate, not a cessation of activity. Therefore, these results suggest that another current underlies the cessation of activity. Modulation of this current must occur before, or initially override, the increase in I_{SOC} activity, to stop the firing. I_{SOC} must eventually dominate, to produce the increase in firing frequency seen during the sustained response phase. We designate the new current I_d. Therefore, it appears that at least three individual currents act coordinately to regulate AP firing in GT1 cells: I_{SOC}, I_{SK}, and I_d.

In further experiments, the Ca^{2+} buffer BAPTA was injected into GT1 cells to prevent an increase in $[Ca^{2+}]_i$ during the GnRH response. This abolished the spike and plateau rise in $[Ca^{2+}]_i$ (Fig. 5*B*). BAPTA also prevented the GnRH-induced membrane hyperpolarization, confirming the dependence of SK channels on $[Ca^{2+}]_i$ (Fig. 5*A*). Moreover, the transient cessation of AP firing observed in GnRH-stimulated cells with blocked SK channels was also abolished by BAPTA. As shown in Figure 5*A*, there was an increase in AP firing frequency almost immediately after GnRH was applied, in contrast to the experiment shown in Figure 3*A*. This suggests that both I_d and I_{SK} are regulated by $[Ca^{2+}]_i$. By inhibiting both currents, BAPTA reveals the effects of the (now clearly) rapidly activated I_{SOC}.

I_d could be either a Ca^{2+}-inactivated current that is active under basal conditions or a Ca^{2+}-activated, apamin-insensitive outward current. In accordance with the former possibility, we were unable to observe any effect of charybdotoxin or iberiotoxin, two specific blockers of BK-type I_{KCa}, on GnRH-induced electrical activity

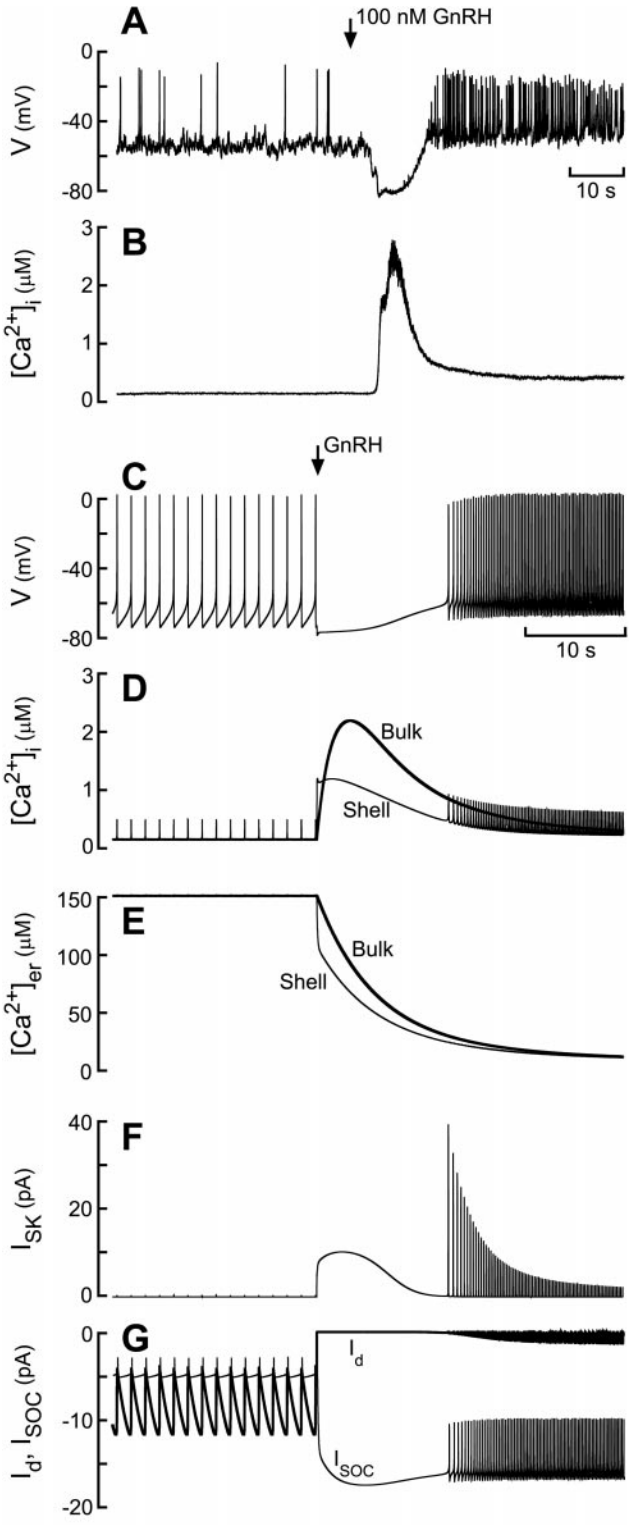

Figure 2. Responses of GT1 neurons and model to GnRH stimulation. Simultaneous V_m (*A*) and $[Ca^{2+}]_i$ (*B*) responses to 100 nM GnRH in GT1 neurons. *C–G*, Model GnRH response, simulated by increasing ER membrane permeability to Ca^{2+} 25-fold. In this and following figures, *heavy* and *light lines* denote bulk and shell compartments, respectively. *C*, V_m response. *D*, $[Ca^{2+}]_i$ and $[Ca^{2+}]_{er}$ (*E*) response. *F*, I_{SK} and I_{SOC} (*G*, *light line*) and I_d (*G, heavy line*) membrane current responses. Calibration in *A* applies to *A* and *B*, and in *C* applies to *C–G*.

(Van Goor et al., 1999a). If present in GT1 cells, two other Ca^{2+}-activated channels, chloride and nonselective, would depolarize cells under our recording conditions. At the present time, we do not have specific information regarding the identity of Ca^{2+}-

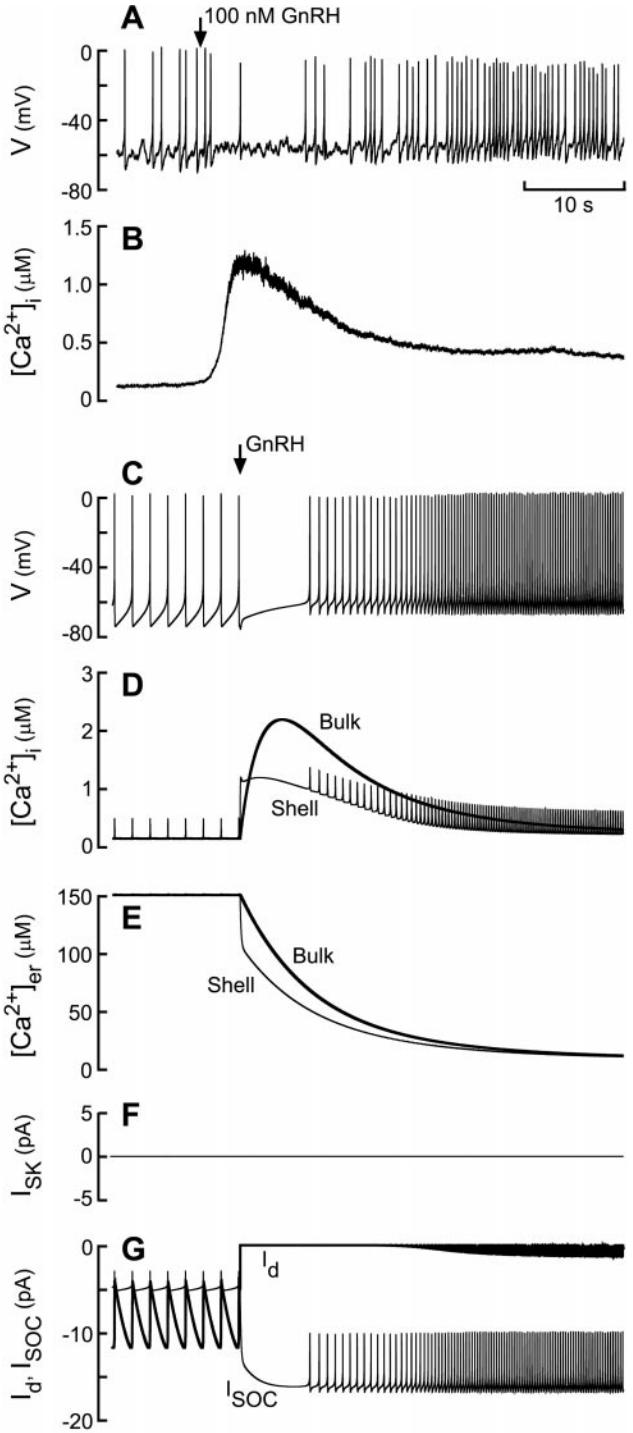

Figure 3. Responses of GT1 neurons and model to addition of GnRH during blockade of SK channels by apamin. Simultaneous V_m (*A*) and $[Ca^{2+}]_i$ (*B*) responses to 100 nM GnRH in GT1 neurons during constant perfusion with 100 nM apamin. *C–G*, Model simulations of GnRH plus apamin response. Apamin was simulated by setting the conductance of I_{SK} to zero. GnRH was simulated as in Figure 2. Calibration in *A* applies to all traces.

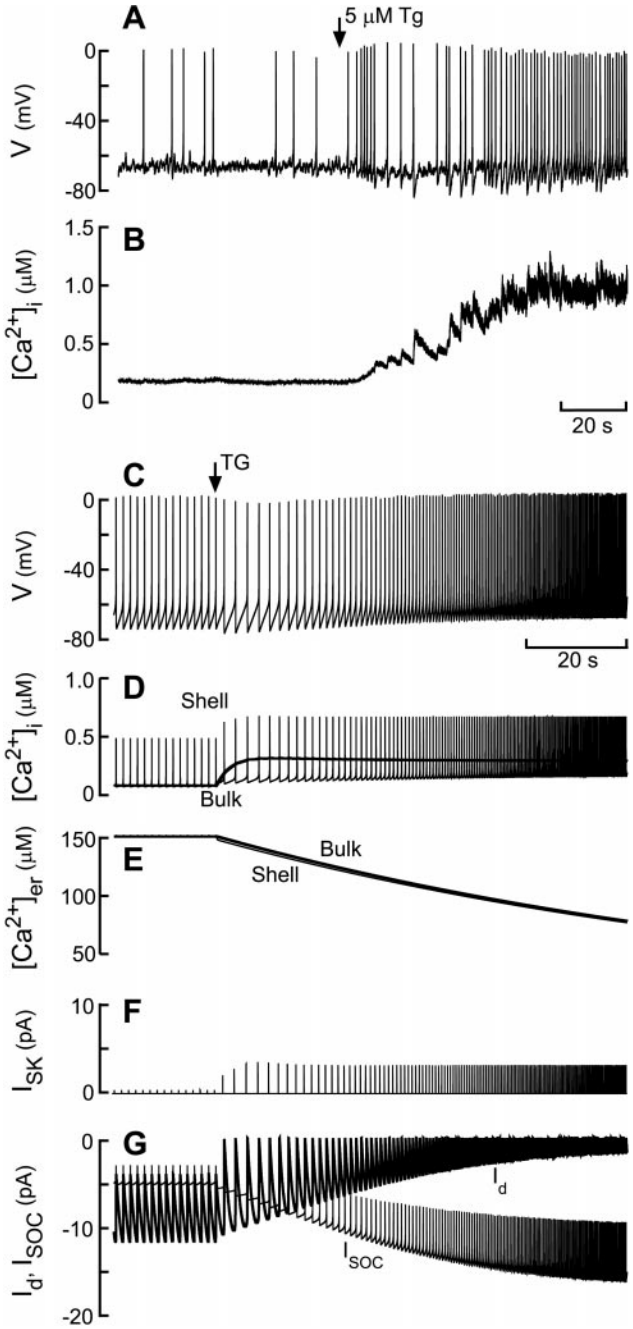

Figure 4. Responses of GT1 neurons and model to addition of endoplasmic reticulum Ca^{2+}-ATPase pump blocker thapsigargin (Tg). Simultaneous V_m (*A*) and $[Ca^{2+}]_i$ (*B*) responses to 5 μM Tg in GT1 neurons. *C–G*, Model simulations of GnRH plus Tg response. Tg was simulated by setting the SERCA pump rates to zero. Calibration in *A* applies to *A* and *B*, and in *C* applies to *C–G*.

inactivated I_d. However, Vitalis et al. (2000) have reported recently that the olfactory subtype of CNG channels is expressed in GT1 cells. These channels have a preference for cAMP over cGMP (Wei et al., 1998) and are inhibited by $[Ca^{2+}]_i$ either directly (Finn et al., 1996; Wei et al., 1998) or indirectly via modulation of AC activity (Hurley, 1999). Consistent with these findings, forskolin, an AC activator, caused an increase in AP frequency with no cessation in firing, no hyperpolarization, and no change in AP amplitude (Fig. 6*A*), whereas $[Ca^{2+}]_i$ rose very slightly (Fig. 6*B*).

Model simulations

Figure 2*C* shows that the model fires spontaneous AP at a frequency of ~0.7 Hz, similar to the average value observed in GT1 cells. During basal activity, bulk $[Ca^{2+}]_i$ ($[Ca^{2+}]_{ib}$) is constant (on the scale shown; Fig. 2*D*) as in the experimental trace (Fig. 2*B*). However, shell $[Ca^{2+}]_i$ ($[Ca^{2+}]_{is}$) shows excursions of ~0.5 μM, coincident with each AP, representing influx of Ca^{2+} during a single spike. The rise in $[Ca^{2+}]_{is}$ is brief because the compartment is small, and the effects of plasma membrane pumps and diffusion into the bulk compartment act rapidly to lower $[Ca^{2+}]_i$.

The model also simulates GnRH-induced store emptying and the consequent effects on plasma membrane electrical activity (Fig. 2*C,D*), when the permeability (p in the equations for j_{relx}; see

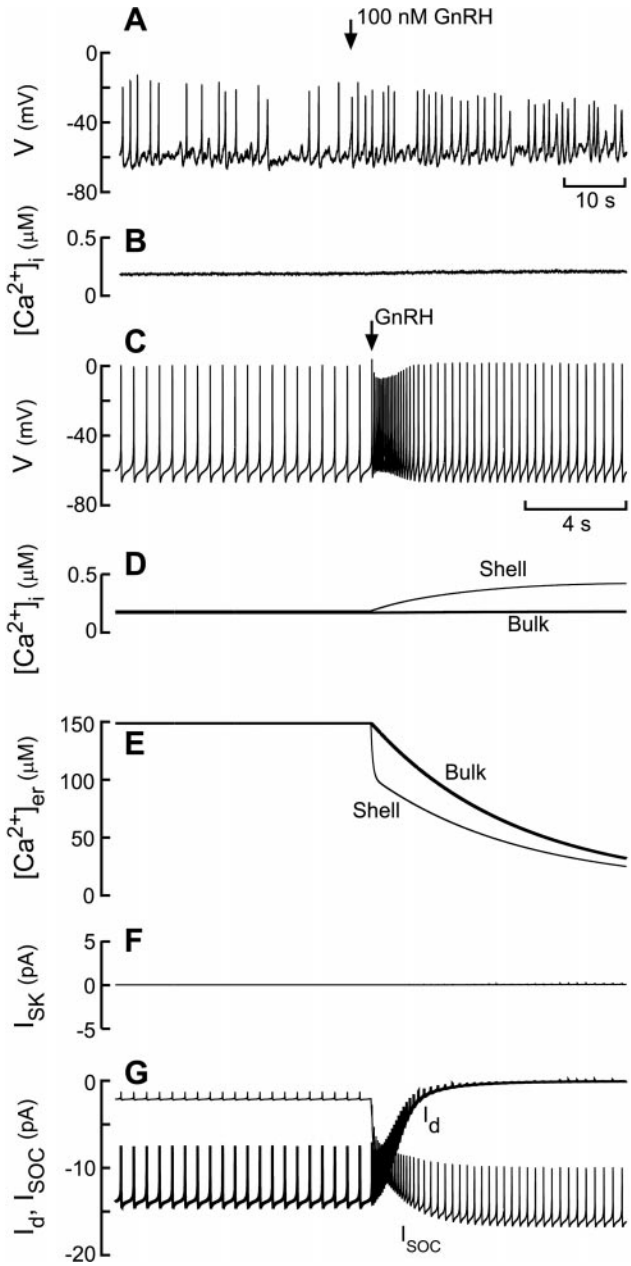

Figure 5. Responses of GT1 neurons and model to GnRH stimulation during $[Ca^{2+}]_i$ buffering with BAPTA. Simultaneous V_m (*A*) and $[Ca^{2+}]_i$ (*B*) responses to 100 nM GnRH in GT1 neurons with $[Ca^{2+}]_i$ clamped to ~200 nM. *C–G*, Model simulations of GnRH plus BAPTA response. BAPTA was simulated by setting the fraction of free cytosolic Ca^{2+} (f_{cyt}) to 1×10^{-5}. Calibration in *A* applies to *A* and *B*, and in *C* applies to *C–G*.

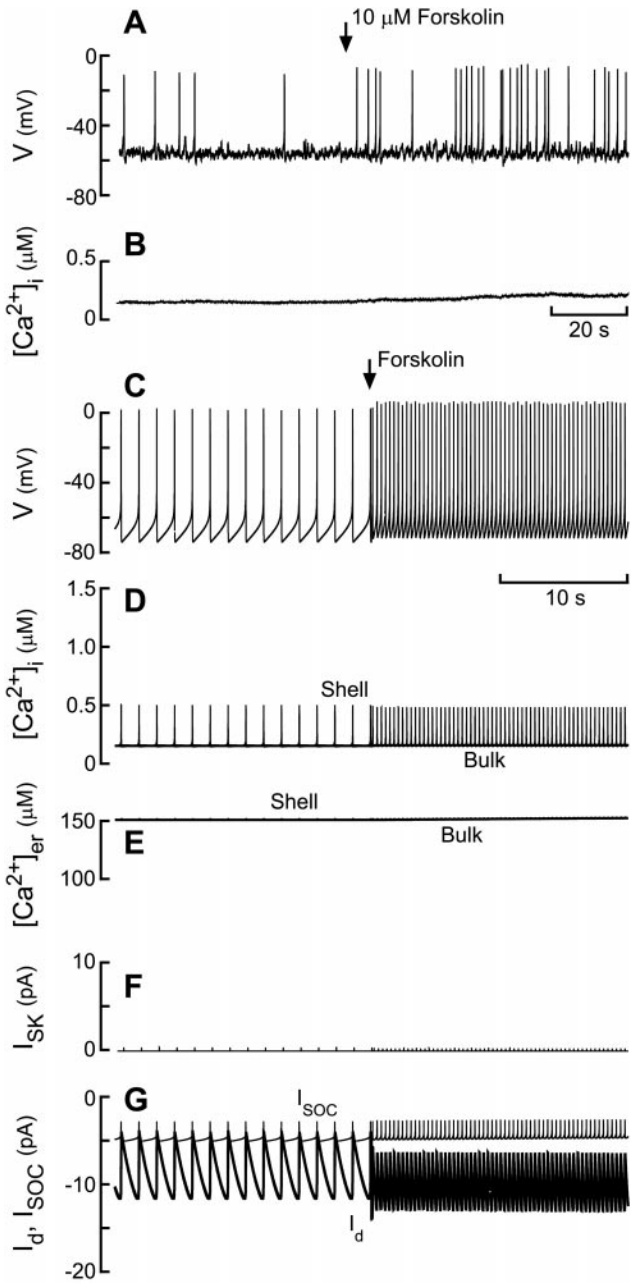

Figure 6. Responses of GT1 neurons and model to activation of adenylyl cyclase by forskolin. Simultaneous V_m (*A*) and $[Ca^{2+}]_i$ (*B*) responses to 10 μM forskolin in GT1 neurons. *C–G*, Model simulations of forskolin response. Forskolin was simulated by a threefold increase in the conductance of I_d. Calibration in *A* applies to *A* and *B*, and in *C* applies to *C–G*.

Appendix) of the ER membrane for Ca^{2+} flux is increased 25-fold. This change is applied equally in both the shell and bulk compartments. In response, $[Ca^{2+}]_{ib}$ rises rapidly to a peak slightly >2 μM, then declines more slowly to a very slowly decaying plateau (Fig. 2*D*). $[Ca^{2+}]_{is}$ also rises rapidly in response to GnRH, but the rise is limited because of plasma membrane pumping. The spike rise in model $[Ca^{2+}]_i$ causes membrane hyperpolarization (Fig. 2*C*) and a temporary cessation of AP firing, as in the experimental trace (Fig. 2*A*). We found that with the parameters required to simulate the pattern of AP firing (our primary focus), the model exhibited a relatively low interspike potential (although within the range observed experimentally; see Fig. 4*A*), which means that it tends to have a more modest GnRH-induced hyperpolarization than typically seen in experiments. However, the cause of the hyperpolarization is well characterized experimentally (activation of I_{SK}; see Fig. 3*A* and Van Goor et al., 1999a). The mechanism underlying the hyperpolarization in the model is the same (see below), so the difference is only quantitative and does not indicate an alternative process.

Finally, Figure 2*E* shows that the shell and bulk ER $[Ca^{2+}]$ ($[Ca^{2+}]_{ers}$ and $[Ca^{2+}]_{erb}$, respectively) are essentially constant during the prestimulus period but that both fall rapidly after application of GnRH. $[Ca^{2+}]_{ers}$ falls slightly faster initially, but both compartments of the store are essentially empty within 20 sec of stimulation. This is consistent with the failure of ionomycin to elicit additional $[Ca^{2+}]_i$ rises when added shortly after GnRH in GT1 cells (data not shown).

Figure 2, *F* and *G*, shows the ionic currents that are principally responsible for controlling plasma membrane excitability and the pattern of AP firing in the GT1 cell model. During basal activity there is no significant activation of I_{SK} (Fig. 2*F*), which is consistent with the lack of effect of apamin on spontaneous AP activity (Van

Goor et al., 1999a). During the spike phase of the $[Ca^{2+}]_i$ response, sustained I_{SK} is evoked, reaching a peak of ~12 pA and causing the transient membrane hyperpolarization shown in Figure 2*C*. The current declines as $[Ca^{2+}]_{is}$ falls, but when AP firing resumes, the residual activation of I_{SK} leads to large current deflections during each spike because of the change in K^+ driving force.

In the model, I_{SOC} is partially activated under basal conditions (Fig. 2*G, light trace*). In response to GnRH, rapid emptying of the ER stores further activates I_{SOC}, reaching a peak of approximately −18 pA. The current then decreases slightly as the driving force for Ca^{2+} falls with V_m depolarization. However, although I_{SOC} is activated, AP firing does not resume until the I_{SK} decays sufficiently for I_{SOC} to dominate. The coordinate actions of I_{SOC} and I_{SK} alone are sufficient to explain some effects of GnRH on electrical activity and Ca^{2+} signaling. However, in the absence of I_d, AP firing frequency after the $[Ca^{2+}]_i$ spike is much greater than the observed experimental range (data not shown). Such rapid firing is further evidence that a third pacemaker current is required; this current must be modulated to compensate for the activation of I_{SOC}. Thus, in addition to the qualitative evidence for I_d provided by the experiments described above, quantitative evidence that such a current is necessary to explain the response to GnRH is provided by the model.

Analysis of the experimental records suggests that I_d is inactivated by $[Ca^{2+}]_i$ (see above), and model simulations support this hypothesis. GnRH-induced store emptying raises $[Ca^{2+}]_{is}$ and inactivates I_d, compensating for the concurrent (although slower) activation of I_{SOC} (Fig. 2*G*). These bidirectional effects result in AP firing frequencies within the experimental range (Fig. 2).

The model simulation of the response to GnRH, during exposure to apamin, is shown in Figure 3*C–G*. The effects of apamin were simulated by setting the conductance of I_{SK} to zero (Fig. 3*F*). This has no effect on the pre-GnRH AP firing frequency (compare Fig. 2*C*), consistent with experimental results discussed above. Also, under these conditions GnRH application causes no membrane hyperpolarization (Fig. 3*C*), demonstrating that inactivation of I_d cannot account for this effect, and no change in the rate of store depletion (Fig. 3*D,E*). Finally, the model is able to mimic the cessation of AP activity observed experimentally in cells with blocked SK channels.

Figure 3*G* suggests an explanation for why AP firing was briefly halted in the absence of any I_{SK}. When GnRH is applied, I_d quickly inactivates because of the rapid rise in $[Ca^{2+}]_{is}$. On the other hand, I_{SOC} activates more gradually, as the ER depletes with a slower time course. The cessation of firing in the model is thus a result of differences in the relative time courses of the changes in $[Ca^{2+}]_i$ levels in the cytosolic and ER pools and hence, the currents they regulate.

The effects of Tg were simulated by setting the SERCA pump rates to zero in both the shell and bulk compartments. This causes an initial slowing of the firing frequency and hyperpolarizes the nadir of the spikes (Fig. 4*C*). Subsequently, the firing rate increases beyond the prestimulus level. $[Ca^{2+}]_i$ in both cytosolic compartments increases after Tg application (Fig. 4*D*). The value for $[Ca^{2+}]_{ib}$ is lower than that observed in the representative experimental trace (Fig. 4*B*), but it is within the range observed from all Tg experiments (data not shown). $[Ca^{2+}]_{er}$ decreases more slowly with Tg application than with GnRH (compare Figs. 2*E,* 4*E*), as expected from the slow leak of Ca^{2+} induced by Tg relative to the rapid store emptying induced by IP_3. The increase in $[Ca^{2+}]_{is}$ activates I_{SK} modestly (Fig. 4*F*), consistent with the effects of apamin on the firing frequency observed experimentally (Van Goor et al., 1999a). Figure 4*G* shows the pattern of I_{SOC} and I_d after Tg application. As the store (specifically the shell ER) empties, I_{SOC} is slowly activated. At the same time, the rise in $[Ca^{2+}]_i$ (specifically $[Ca^{2+}]_{is}$), which is also slow, inactivates I_d. The two currents essentially switch activity levels, at about the same rate, so there is no cessation of AP firing. I_d decreases more rapidly than I_{SOC} increases, resulting in a slight initial reduction of AP firing frequency immediately after Tg application. After ~20 sec, I_{SOC} dominates I_d sufficiently to cause the firing frequency to increase beyond the prestimulus level.

The effects of BAPTA were simulated by decreasing f_{cyt}, the fraction of free Ca^{2+} in the cytosol, such that $[Ca^{2+}]_{ib}$ does not rise significantly when GnRH is applied (Fig. 5*D, heavy line*). We confirmed that this treatment prevents membrane hyperpolarization and cessation of AP activity in the model as in the experiments (Fig. 5*C*). There is a brief period of rapid firing that was not observed experimentally, suggesting that we have perhaps not fully captured the complexity of $[Ca^{2+}]_i$-induced changes in pacemaker currents (see below). However, after this the firing frequency settles down to a rate moderately faster than before GnRH, consistent with the experimental record. Figure 5*D* shows that BAPTA simulation prevents the brief pulses of $[Ca^{2+}]_{is}$ before GnRH application, but that after GnRH, $[Ca^{2+}]_{is}$ rises slowly, reflecting an inability of the enhanced buffer to completely prevent a rise in $[Ca^{2+}]_i$ in the small-volume shell compartment.

This slow rise in $[Ca^{2+}]_{is}$ is important for the response of the model to GnRH in the presence of BAPTA. Figure 5*G* shows that with GnRH application, I_{SOC} is activated in response to store emptying, but at the same time I_d is slowly decreased by the slow rise in $[Ca^{2+}]_{is}$. Both the rise and its slowness are important—if no rise occurred, I_d would not be inactivated, and the firing frequency would be too high, as in the initial rapid-firing phase. Moreover, because the rise in $[Ca^{2+}]_{is}$ is slow (on approximately the same time scale as I_{SOC} activation), I_d inactivates more slowly than during GnRH (Fig. 2) or GnRH plus apamin (Fig. 3), so there is no cessation of AP activity. Instead, there is a transfer of control of AP activity from I_d to I_{SOC}, with I_{SK} playing no role (Fig. 5*F*). The lack of a rapid firing phase in the experimental data suggests that transfer of control of firing frequency is even more tightly regulated in the cells than is captured by our relatively simple descriptions of the two currents.

As a final test, we asked whether I_d could represent a CNG channel. Specifically, we tested whether the experimental response to forskolin could be modeled by increasing the conductance of I_d. In fact, this causes an increase in firing frequency without a cessation of AP activity, membrane hyperpolarization, or a change in AP amplitude (Fig. 6*C*). $[Ca^{2+}]_i$ in the shell or bulk compartments does not rise significantly (Fig. 6*D*), and $[Ca^{2+}]_{er}$ is unaffected (Fig. 6*E*). I_{SK} and I_{SOC} (Fig. 6*F,G*, respectively) are unaffected by forskolin, and I_d is slightly increased (Fig. 6*G*). This latter effect is solely responsible for the increased AP firing frequency.

DISCUSSION

We have presented here a mathematical model that provides a quantitative description of the regulation of AP pacemaking and the associated $[Ca^{2+}]_i$ signaling in GT1 neurons. The results indicate that a complex interplay of at least three pacemaker currents, modulated by at least two distinct Ca^{2+} pools (cytosol and ER), regulates AP firing in GT1 cells. The pacemaker currents included in the model are I_{SOC}, I_{SK}, and the cAMP-regulated I_d. Spontaneous firing and the associated Ca^{2+} signaling in the model are predominantly controlled by I_d. Increasing the activity of I_d also simulates the experimental response to forskolin-induced activation of AC. In contrast, activation of I_{SOC} by depletion of the intracellular Ca^{2+} pool and I_{SK} by the concomitant rise in $[Ca^{2+}]_i$, as well as a decrease in I_d, is required to mimic the increase in the firing frequency and Ca^{2+} influx observed in cells stimulated with Ca^{2+}-mobilizing agonists.

In general, the expression of I_{SOC} in excitable cells provides a potential mechanism to link AP-driven Ca^{2+} influx with agonist-induced store depletion (Berridge, 1998). In cells with a leaky ER Ca^{2+} pool (i.e., with relatively high basal levels of leak and uptake), the same channels may play a role in the control of pacemaking in spontaneously active cells. Coupled to I_{SK}, such a system should lead to controlled Ca^{2+} influx to replenish the depleted pool. However, from the analysis of the experimental data presented here and published earlier (Van Goor et al., 1999a), no

evidence for a regulatory role of I_{SOC} and I_{SK} in spontaneously active cells was observed. The need for an additional pacemaker current also emerged from our simulations with an early-stage model, which contained only I_{SK} and I_{SOC} as pacemaker currents. In the absence of I_d, such a model was unable to mimic all aspects of spontaneous and agonist-induced AP firing. Furthermore, the integration of I_d helped to mimic the action of AC-coupled receptors in these cells (Martínez de la Escalera et al., 1992b,c).

In our model, control of basal electrical activity is predominantly achieved by I_d, a channel that is activated by cAMP and inhibited by $[Ca^{2+}]_i$. Although we have not recorded I_d experimentally, the CNG channel recently described by Vitalis et al. (2000) in GT1 cells is an obvious candidate. Another, more complex, possibility is that I_d could actually represent $[Ca^{2+}]_i$-mediated inactivation of I_{SOC} (Lewis, 1999). That is, the ER store and $[Ca^{2+}]_i$ would act antagonistically on I_{SOC}, and a separate population of CNG channels would mediate the effects of AC-coupled agonists. We have performed simulations to confirm that this is a viable mechanism. However the model cannot discriminate between the two possible systems because the pacemaker currents (I_{SOC} and I_d) are not well characterized. The model is able to tell us what the characteristics of the currents need to be to generate the observed firing patterns, and the single current (I_{SOC} with inactivation) can produce equivalent results provided it behaves more-or-less like the sum of the two original currents. Without specific experimental characterization of the currents in these cells, the model can only make predictions that can be tested experimentally. We favor separating the channels because: (1) "slow inactivation" of I_{SOC} (Zweifach and Lewis, 1995b; Liu et al., 1998) is too slow for the effects necessary in our model, and "fast inactivation" of the Ca^{2+}-release activated Ca^{2+} current (CRAC) form of I_{SOC} (Zweifach and Lewis, 1995a) is only marginally active at the interspike potentials in GT1 neurons; and (2) there is experimental evidence for a CNG channel in GT1 neurons (Vitalis et al., 2000). Because we are not aware of any experimental evidence for cAMP activation of I_{SOC}, a second channel is still necessary. Therefore two currents, as described here, is the simplest form, and additional experimental evidence would be necessary to support a more complex system.

When integrated with I_d, two other channels, I_{SK} and I_{SOC}, play specific roles in control of pacemaking. In our model, I_{SK} is not significantly activated in spontaneously active cells, and I_{SOC}, although modestly activated, provides only a fairly constant background conductance. The background activity of I_{SOC} is consistent with findings by Bennett et al. (1998) in PC12 cells and also with our observation of the relatively rapid effects of Tg on AP firing frequency, which suggests that little store emptying is needed for an increase in I_{SOC}. This could easily be achieved if I_{SOC} is already partially activated.

The real importance of I_{SOC} is in mimicking the action of Ca^{2+}-mobilizing agonists. In our model, an increase in AP firing frequency in response to GnRH is driven primarily by I_{SOC}, with I_d and I_{SK} playing regulatory roles. I_{SK} generates the membrane hyperpolarization, although it is not clear whether this has any physiological function, and keeps a partial brake on AP frequency once firing resumes. I_d is rapidly inactivated by the spike $[Ca^{2+}]_i$ rise, passing control of AP firing over to I_{SOC}. As the store refills slowly after removal of GnRH, I_{SOC} gradually relinquishes control back to I_d (data not shown).

Store-operated channels have been studied most intensively in nonexcitable cells with much less attention given to their presence and role in excitable cells. Here we have shown how I_{SOC} can integrate the state of store Ca^{2+} content into excitable membrane activity. During the response to GnRH, the cytosolic and ER Ca^{2+} stores act in opposite directions on membrane excitability. GnRH causes a rise in $[Ca^{2+}]_i$ which acts to depress membrane activity by increasing I_{SK} activation and inactivating I_d, whereas the depleted ER pool increases I_{SOC} activity to increase membrane activity. In other situations the two pools may work in concert. For example, in the model we allow a low level of I_{SOC} activation at rest, so that if a depolarizing stimulus were applied, there would be an increase in AP activity that would increase $[Ca^{2+}]_i$, some of which would be taken up into the ER. The increase in $[Ca^{2+}]_{er}$ would cause I_{SOC} to be reduced and, together with a $[Ca^{2+}]_i$-induced decrease in I_d, would counteract the depolarizing stimulus.

The two cases in which the cytosolic and ER Ca^{2+} pools act either in opposition or together in regulating membrane electrical activity suggest a general rule for Ca^{2+} handling: in the absence of a Ca^{2+}-mobilizing agonist, the cytosolic and ER pools rise and fall together in response to changes in Ca^{2+} entry (regulated by membrane electrical activity in these cells). For both pools a rise in $[Ca^{2+}]$ has an inhibitory effect on electrical activity (Chay, 1997). However, store-emptying breaks the connection, and the pools work antagonistically until the store is refilled.

In the model, the Ca^{2+}-mobilizing agonist (GnRH), transiently shuts off I_d and stimulates I_{SOC}, whereas activation of I_d simulates the experimental response to an AC activator, supporting I_d being the CNG channel found by Vitalis et al. (2000) in GT1 neurons. The model also suggests that in contrast to Ca^{2+}-mobilizing agonists, which modulate all three pacemaker currents, AC-coupled agonists increase AP activity by modulating I_d alone and thus act independently of the ER. This suggests that AC-coupled agonists act to a greater degree on $[Ca^{2+}]_i$ local to the plasma membrane, compared with calcium-mobilizing agonists, which act globally through emptying of the ER store. These differences may reflect differential roles of the respective agonists on the patterns of secretion and protein synthesis (Dolmetsch et al., 1998).

In the model, it was necessary to compartmentalize the cytosolic and ER Ca^{2+} pools to get the appropriate changes in the pacemaker currents after agonist–drug addition. The model suggests that the region of the cytosol immediately adjacent to the plasma membrane has a degree of functional separation from the interior cytosol. This separation allows $[Ca^{2+}]_i$ in this region to be more dynamic than, and act somewhat independently of, bulk $[Ca^{2+}]_i$. Similarly the ER in this region may also be more dynamic than the bulk ER, allowing rapid modulation of I_{SOC} and thus electrical activity. Broad et al. (1999) and Gregory et al. (1999) have also reported evidence supporting the concept of specialized Ca^{2+} signaling in the periphery of the cell. Moreover, a close functional connection between the shell ER and I_{SOC} is consistent with several recent reports indicating a physical connection between IP_3Rs and I_{SOC} channels (Kiselyov et al., 1998, 1999; Boulay et al., 1999; Ma et al., 2000) (also see Putney, 1999).

The shell Ca^{2+} pools cannot, however, function completely independently of their bulk counterparts. In the case of the ER this raises an intriguing possibility. The model shows that the activity of I_{SOC} can be modulated on the time scale of the shell ER. Because there is still slow communication between ER compartments, I_{SOC} activity can also be modulated on the time scale of the bulk ER, which is on the order of 10–20 min in the absence of elevated $[IP_3]$. Therefore, the ER can potentially regulate plasma membrane excitability on both fast (seconds) and slow (tens of minutes) time scales.

In conclusion, the experimental and theoretical results present here provide a model for spontaneous electrical activity of neuroendocrine cells that also accommodates the integration of two major receptor pathways, Ca^{2+}-mobilizing and AC-coupled, in control of spontaneous electrical activity. The model suggests that in spontaneously active cells, basal AC activity, possibly activated by voltage-gated Ca^{2+} influx, generates cAMP and thus activation of CNG-like I_d channels. Control of spontaneous electrical activity and the $[Ca^{2+}]_i$-dependent AC is achieved by an increase in localized $[Ca^{2+}]_i$, which transiently inactivates I_d. Activation of Ca^{2+}-mobilizing receptors also leads to inhibition of I_d but stimulates I_{SOC}, which is responsible for reinitiation of electrical activity, whereas agonist-induced activation of AC facilitates I_d independently of the status of I_{SOC}. At the same time, I_{SK} protects the cells from Ca^{2+} overload when the pacemaking is predominantly controlled by I_{SOC}.

APPENDIX

The appendix for this manuscript may be viewed at http://www.jneurosci.org.

REFERENCES

Al-Damluji S, Krsmanovic LZ, Catt KJ (1993) High-affinity uptake of noradrenaline in postsynaptic neurones. Br J Pharmacol 109:299–307.

Bennett DL, Bootman MD, Berridge MJ, Cheek TR (1998) Ca^{2+} entry into PC12 cells initiated by ryanodine receptors or inositol 1,4,5-trisphosphate receptors. Biochem J 329:349–357.

Berridge MJ (1998) Neuronal calcium signaling. Neuron 21:13–26.

Bertram R, Smolen P, Sherman A, Mears D, Atwater I, Martin F, Soria B (1995) A role for calcium release-activated current (CRAC) in cholinergic modulation of electrical activity in pancreatic β-cells. Biophys J 68:2323–2332.

Boulay G, Brown DM, Qin N, Jiang M, Dietrich A, Zhu MX, Chen Z, Birnbaumer M, Mikoshiba K, Birnbaumer L (1999) Modulation of Ca^{2+} entry by polypeptides of the inositol 1,4,5-trisphosphate receptor (IP3R) that bind transient receptor potential (TRP): evidence for roles of TRP and IP3R in store depletion-activated Ca^{2+} entry. Proc Natl Acad Sci USA 96:14955–14960.

Broad LM, Armstrong DL, Putney Jr JW (1999) Role of the inositol 1,4,5-trisphosphate receptor in Ca^{2+} feedback inhibition of calcium release-activated calcium current (I_{CRAC}). J Biol Chem 274:32881–32888.

Chay TR (1997) Effects of extracellular calcium on electrical bursting and intracellular and luminal calcium oscillations in insulin secreting pancreatic β–cells. Biophys J 73:1673–1688.

Constantin JL, Charles AC (1999) Spontaneous action potentials initiate rhythmic intercellular calcium waves in immortalized hypothalamic (GT1–1) neurons. J Neurophysiol 82:429–435.

Csordás G, Thomas AP, Hajnóczky G (1999) Quasi-synaptic calcium signal transmission between endoplasmic reticulum and mitochondria. EMBO J 18:96–108.

Dolmetsch RE, Xu K, Lewis RS (1998) Calcium oscillations increase the efficiency and specificity of gene expression. Nature 392:933–936.

Finn JT, Grunwald ME, Yau K-W (1996) Cyclic nucleotide-gated ion channels: An extended family with diverse functions. Annu Rev Physiol 58:395–426.

Fomina AF, Nowycky MC (1999) A current activated on depletion of intracellular Ca^{2+} stores can regulate exocytosis in adrenal chromaffin cells. J Neurosci 19:3711–3722.

Gregory RB, Wilcox RA, Berven LA, van Straten NCR, van der Marel GA, van Boom JH, Barritt GJ (1999) Evidence for the involvement of a small subregion of the endoplasmic reticulum in the inositol trisphosphate receptor-induced activation of Ca^{2+} inflow in rat hepatocytes. Biochem J 341:401–408.

Hurley JH (1999) Structure mechanism, and regulation of mammalian adenylyl cyclase. J Biol Chem 274:7599–7602.

Jarry H, Leonhardt S, Wuttke W (1990) A norepinephrine-dependent mechanism in the preoptic/anterior hypothalamic area but not in the mediobasal hypothalamus is involved in the regulation of the gonadotropin-releasing hormone pulse generator in ovariectomized rats. Neuroendocrinology 51:337–344.

Kao JPY (1994) Practical aspects of [Ca^{2+}] with fluorescent indicators. Methods Cell Biol 40:155–181.

Kiselyov K, Xu X, Mozhayeva G, Kuo T, Pessah I, Mignery G, Zhu X, Birnbaumer L, Muallem S (1998) Functional interaction between $InsP_3$ receptors and store-operated Htrp3 channels. Nature 396:478–482.

Kiselyov K, Mignery GA, Zhu MX, Muallem S (1999) The N-terminal domain of the IP_3 receptor gates store-operated hTrp3 channels. Molecular Cell 4:423–429.

Knobil E (1980) The neuroendocrine control of the menstrual cycle. Recent Prog Horm Res 36:53–88.

Krsmanovic LZ, Stojilkovic SS, Balla T, Al-Damluji S, Weiner RI, Catt KJ (1991) Receptors and neurosecretory actions of endothelin in hypothalamic neurons. Proc Natl Acad Sci USA 88:11124–11128.

Krsmanovic LZ, Stojilkovic SS, Merelli F, Dufour SM, Virmani MA, Catt KJ (1992) Calcium signaling and episodic secretion of gonadotropin-releasing hormone in hypothalamic neurons. Proc Natl Acad Sci USA 89:8462–8466.

Krsmanovic LZ, Stojilkovic SS, Mertz LM, Tomic M, Catt KJ (1993) Expression of gonadotropin-releasing hormone receptors and autocrine regulation of neuropeptide release in immortalized hypothalamic neurons. Proc Natl Acad Sci USA 90:3908–3912.

Kusano K, Fueshko S, Gainer H, Wray S (1995) Electrical and synaptic properties of embryonic luteinizing hormone-releasing hormone neurons in explant cultures. Proc Natl Acad Sci USA 92:3918–3922.

Lewis RS (1999) Store-operated calcium channels. Adv Second Messenger Phosphoprotein Res 33:279–307.

Liu X, O'Connell A, Ambudkar IS (1998) Ca^{2+}-dependent inactivation of a store-operated Ca^{2+} current in human submandibular gland cells. J Biol Chem 273:33295–33304.

Ma H-T, Patterson RL, van Rossum DB, Birnbaumer L, Mikoshiba K, Gill DL (2000) Requirement of the inositol trisphosphate receptor for activation of store-operated Ca^{2+} channels. Science 287:1647–1651.

Martínez de la Escalera G, Choi ALH, Weiner RI (1992a) Generation and synchronization of gonadotropin-releasing hormone (GnRH) pulses: intrinsic properties of the GT1–1 GnRH neuronal cell line. Proc Natl Acad Sci USA 89:1852–1855.

Martínez de la Escalera G, Choi ALH, Weiner RI (1992b) β_1-adrenergic regulation of the GT_1 gonadotropin-releasing hormone (GnRH) neuronal cell lines: stimulation of GnRH release via receptors positively coupled to adenylate cyclase. Endocrinology 131:1397–1402.

Martínez de la Escalera G, Gallo F, Choi ALH, Weiner RI (1992c) Dopaminergic regulation of the GT_1 gonadotropin-releasing hormone (GnRH) neuronal cell lines: stimulation of GnRH release via D_1-receptors positively coupled to adenylate cyclase. Endocrinology 131:2965–2971.

Mellon PL, Windle JJ, Goldsmith PC, Padula CA, Roberts JL, Weiner RI (1990) Immortalization of hypothalamic GnRH neurons by genetically targeted tumorigenesis. Neuron 5:1–10.

Parekh AB, Penner R (1997) Store depletion and calcium influx. Physiol Rev 77:901–930.

Pivovarova NB, Hongpaisan J, Andrews SB, Friel DD (1999) Depolarization-induced mitochondrial Ca accumulation in sympathetic neurons: Spatial and temporal characteristics. J Neurosci 19:6372–6384.

Putney Jr JW (1999) TRP, inositol 1,4,5-trisphosphate receptors, and capacitative calcium entry. Proc Natl Acad Sci USA 96:14669–14671.

Rizzuto R, Brini M, Murgia M, Pozzan T (1993) Microdomains with high Ca^{2+} close to IP_3-sensitive channels that are sensed by neighboring mitochondria. Science 262:744–747.

Spergel DJ, Krüth U, Hanley DF, Sprengel R, Seeburg PH (1999) GABA- and glutamate-activated channels in green fluorescent protein-tagged gonadotropin-releasing hormone neurons in transgenic mice. J Neurosci 19:2037–2050.

Terasawa E, Schanhofer WK, Keen KL, Luchansky L (1999) Intracellular Ca^{2+} oscillations in luteinizing hormone-releasing hormone neurons derived from the embryonic olfactory placode of the rhesus monkey. J Neurosci 19:5898–5909.

Van Goor F, Krsmanovic LZ, Catt KJ, Stojilkovic SS (1999a) Coordinate regulation of gonadotropin-releasing hormone neuronal firing patterns by cytosolic calcium and store depletion. Proc Natl Acad Sci USA 96:4101–4106.

Van Goor F, Krsmanovic LZ, Catt KJ, Stojilkovic SS (1999b) Control of action potential-driven calcium influx in GT1 neurons by the activation status of sodium and calcium channels. Mol Endocrinol 13:587–603.

Van Goor F, LeBeau AP, Krsmanovic LZ, Sherman A, Catt KJ, Stojilkovic SS (2000) Amplitude-dependent spike-broadening and enhanced Ca^{2+} signaling in GnRH-secreting neurons. Biophys J 79: 1310–1323.

Vitalis EA, Costantin JL, Tsai P-S, Sakakibara H, Paruthiyil S, Iiri T, Martini J-F, Taga M, Choi ALH, Charles AC, Weiner RI (2000) Role of the cAMP signaling pathway in the regulation of gonadotropin-releasing hormone secretion in GT1 cells. Proc Natl Acad Sci USA 97:1861–1866.

Wei J-Y, Samanta Roy D, Leconte L, Barnstable CJ (1998) Molecular and pharmacological analysis of cyclic nucleotide-gated channel function in the central nervous system. Prog Neurobiol 56:37–64.

Wetsel WC, Valença MM, Merchenthaler I, Liposits Z, José López F, Weiner RI, Mellon PL, Negro-Vilar A (1992) Intrinsic pulsatile secretory activity of immortalized luteinizing hormone-releasing hormone-secreting cells. Proc Natl Acad Sci USA 89:4149–4153.

Zweifach A, Lewis RS (1995a) Rapid inactivation of depletion-activated calcium current (I_{CRAC}) due to local calcium feedback. J Gen Physiol 105:209–226.

Zweifach A, Lewis RS (1995b) Slow calcium-dependent inactivation of depletion-activated calcium current. J Biol Chem 270:14445–14451.